PHYSICAL REVIEW B
CONDENSED MATTER

THIRD SERIES, VOLUME 43, NUMBER 1 PART A 1 JANUARY 1991

Deuteron relaxation in HD$-n$-D_2 mixtures

Joseph Ganem* and R. E. Norberg
Department of Physics, Washington University, St. Louis, Missouri 63130-4899
(Received 26 July 1990)

Deuteron magnetic resonance at 55 MHz was performed on solid and liquid mixtures of HD$-n$-D_2. In liquid mixtures, the lack of rapid spin diffusion results in separate spin-lattice relaxation times (T_1) for HD, ortho-D_2, and para-D_2. For solid mixtures, a common T_1 for deuterons from all the molecular species is observed. Deuteron relaxation times T_1 and T_2 between 8 and 16 K are reported. Between 8 and 11 K there is little temperature dependence of either relaxation time. The concentration of para-D_2 controls T_1 but T_2 has little dependence on sample composition because of a self-narrowing effect in HD. Predictions of a model, developed by Drabold and Fedders, are compared to the T_1 results. The self-narrowing of HD is understood as arising from an increase in the intermolecular proton-proton flip-flop rate as the temperature is lowered. Above 11 K and until the melting point is reached, T_1 and T_2 increase with temperature in a manner determined by sample composition and the activation energy for self-diffusion. In this temperature regime T_1 and T_2 are related by a simple scaling relationship and analysis of these times yields the activation energy for self-diffusion which depends on sample composition. Extrapolation to the limiting cases of pure n-D_2 and pure HD determines their activation energies for self-diffusion to be 308 and 237 K, respectively. The relationship between T_1 and T_2 is understood in terms of a model developed by Bloom which is modified to account for the intrinsic relaxation of HD.

I. INTRODUCTION

This paper reports measurements of longitudinal and transverse nuclear-spin relaxation times of deuterons in solid mixtures of HD–n-D_2. Previous work has reported on proton relaxation in ortho-H_2–para-H_2 mixtures[1–3] and HD–n-H_2 mixtures.[4–6] Deuteron magnetic resonance (DMR) on solid mixtures of ortho-D_2–para-D_2 also have been reported.[7–10] There are, however, little data on DMR in HD–n-D_2 mixtures, especially at high magnetic fields.[11] In the present work, deuteron relaxation was examined in n-D_2 and in solid mixtures of HD–n-D_2. The measurements were performed at a much higher Larmor frequency than earlier work. The results provide an important complement to the other studies of hydrogen mixtures as well as a test of the Larmor frequency dependence of the relaxation.

This paper is organized into four main sections. Section II is an overview of the data and its important features. Then a theoretical background, Sec. III, will be given and a model for understanding spin-lattice relaxation in HD–n-D_2 mixtures will be presented. Section IV describes the experimental setup and measurement methods. Section V is a discussion of the results and conclusions.

II. OVERVIEW OF THE DATA

Relaxation times as a function of temperature for four solid mixtures are shown in Fig. 1. Shown in Fig. 1(a) are longitudinal relaxation times (T_1), and in Fig. 1(b) are transverse relaxation times (T_2). As in earlier reported work on deuterium in the hcp phase,[7] two distinct temperature regions in the solid are identified. The rigid lattice (below 11 K) is characterized by deuteron relaxation times with little temperature dependence. The rigid lattice T_1 depends on the concentration of para-D_2 and in the samples studied varies between 1 and 20 sec. There is little variation between samples of T_2 in the rigid lattice which is about 0.3 msec. In the second region between 11 K and the melting point, thermally activated self-diffusion affects the relaxation times. T_1 shows dramatic dependence on both temperature and para-D_2 concentration. T_1 can become several hundreds of seconds in samples with low enough para-D_2 concentrations. T_2 can increase to almost a second and shows a functional relation similar to T_1.

A characteristic of the solid phase in a HD–n-D_2 mixture is a common T_1 shared by the deuterons of all three molecular species. In the liquid phase, deuterons in the HD, ortho-D_2, and para-D_2 relax separately with very

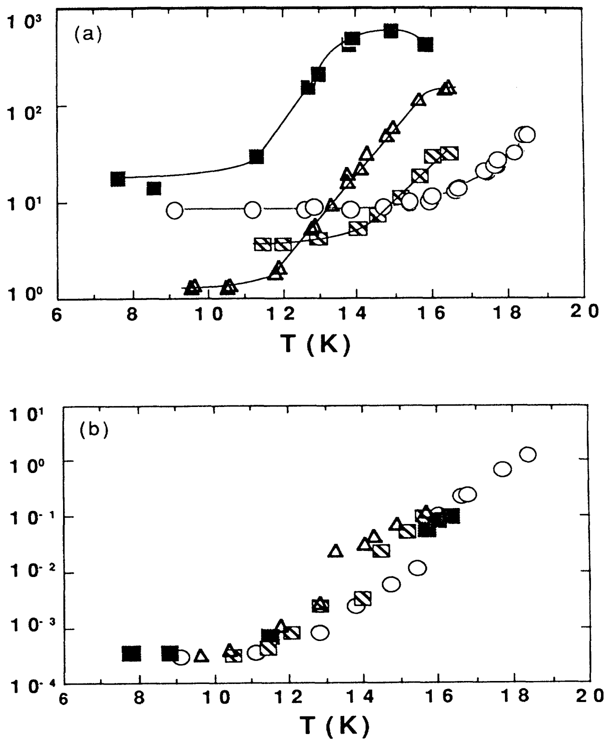

FIG. 1. Relaxation times as function of temperature for four of the solid mixtures studied. The open circles are times for n-D_2, the hatched squares are for the (65% HD)/(35% n-D_2) mixture, the open triangles are the (83% HD)/(17% n-D_2) mixture and the solid squares are the (97% HD)/(3% n-D_2) mixture. (a) longitudinal relaxation times (T_1), (b) transverse relaxation times (T_2).

different T_1's. Figure 2 illustrates the separate deuteron relaxation times in a (65% HD)/(35% n-D_2) liquid mixture. The recovery of the magnetization as a function of time at 20.2 K is shown for D_2 (open circles) and HD (solid squares). Figure 2(a) shows the clearly separate relaxation of ortho-D_2 ($T_1 = 1400$ sec) and HD ($T_1 = 950$ sec). A closeup of the first 2 min of Fig. 2(a) shown in Fig. 2(b) illustrates the initial fast recovery of para-D_2 ($T_1 = 1.1$ sec). In n-D_2, $\frac{5}{6}$ of the total D_2 signal is from ortho-D_2, the remaining $\frac{1}{6}$ is from para-D_2.

In a liquid HD–n-D_2 mixture, the HD and D_2 signals are easy to separate since they account for separate lines in the NMR spectrum. The deuteron resonance in liquid HD is a doublet. Liquid D_2 has a single resonance line slightly offset from the center of the HD doublet. The splitting of the HD resonance arises from an indirect spin-spin coupling between the deuteron and the proton. The spins couple indirectly through the electrons. The mechanism for this interaction was first explained by Ramsey and Purcell.[12] An analogous splitting is not seen for D_2 because this type of interaction only produces observable splittings between inequivalent spins.[13] The splitting (J_{HD}), is independent of the external magnetic field. Beckett[14] reported J_{HD} in liquid HD at 20.5 K as 42.82 ± 0.01 Hz. In this work two measurements of J_{HD} were made for liquid HD. The results, 42.79 ± 0.85 Hz at 20.0 K and 42.85 ± 0.35 Hz at 19.1 K are, to within experimental error, in agreement with Beckett's measurement.

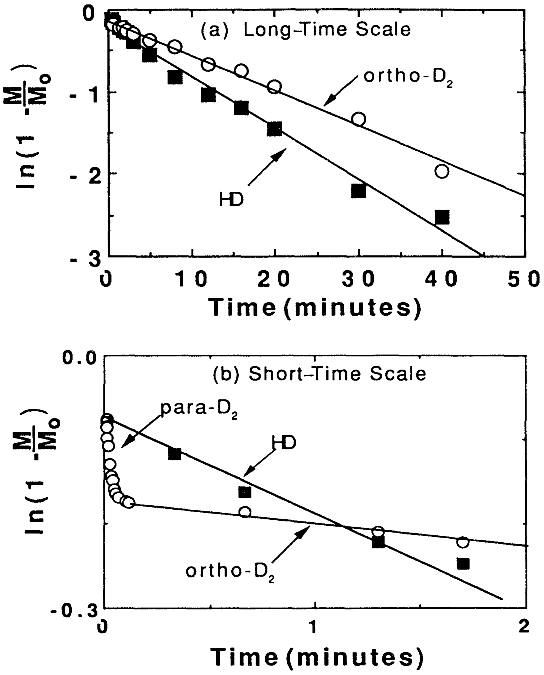

FIG. 2. Recovery of the magnetization for D_2 (open circles) and HD (solid squares) in a (65% HD)/(35% n-D_2) liquid mixture at 20.2 K. (a) The long time scale shows the clearly separate relaxation of the ortho-D_2 ($T_1 = 1400$ sec) and the HD ($T_1 = 950$ sec). (b) A closeup of the first 2 min illustrates the initial fast recovery of the para-D_2 ($T_1 = 1.1$ sec).

Solid HD well below the triple point (16.6 K) has a single resonance line. We observed the transition between the two kinds of resonant structures. Figure 3 shows the line shape of HD as a function of temperature between 14.0 and 16.2 K. The line shapes in Fig. 3 are from a sample consisting of (97% HD)/(3% n-D_2). An unusual feature of the transition of the HD resonance is the initial narrowing of the overall resonant structure[13] as the temperature lowers. If we define the overall width of the HD resonance as the full width at half maximum of the entire resonant structure, this width, about 82 Hz at 16.2 K, remains unchanged for the line shapes at 15.7 and 15.4 K. However, the line shape at 14.0 K shows a single resonance line with a width of 56 Hz. Only at temperatures colder than 14 K does the line begin to broaden. The full width at half maximum is 125 Hz at 12.9 K and in the rigid lattice at 10 K, the line broadens to about 1000 Hz.

III. RELAXATION MECHANISMS IN SOLID HYDROGEN

Gaines and Souers have reviewed[15] the basic relaxation mechanisms that operate in solid hydrogen. Figure 4 illustrates the pathways by which energy is transferred from the deuteron spin system to the lattice. The direct

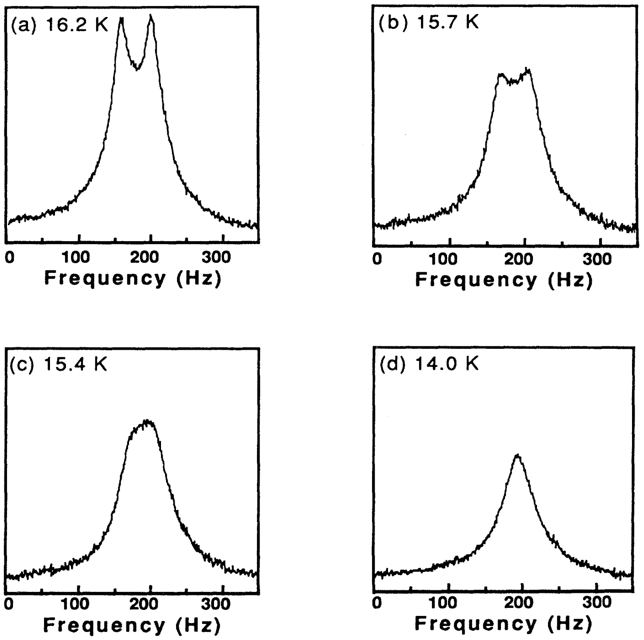

FIG. 3. The evolution of the HD line shape as a function of temperature. As the temperature decreases the overall width of the resonant structure narrows. (a) 16.2 K, (b) 15.7 K, (c) 15.4 K, and (d) 14.0 K.

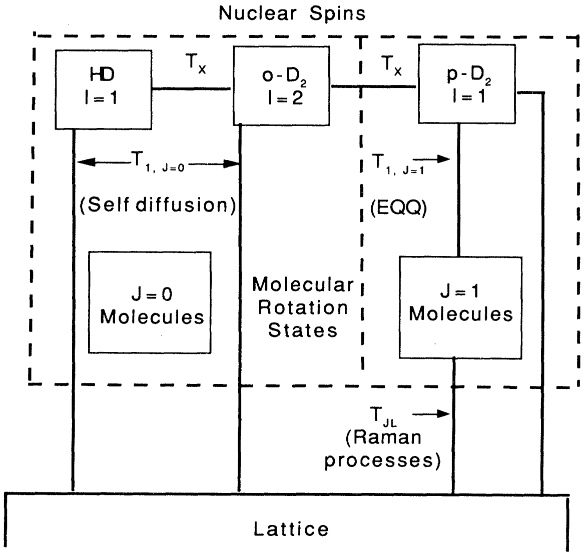

FIG. 4. Diagram illustrating pathways for energy transfer during spin-lattice relaxation in solid HD–n-D$_2$ mixtures. The relative effectiveness of the pathways depends on the temperature. Two temperature regions can be identified: (1) Rigid lattice: $8 < T < 11$ K, no self-diffusion so direct relaxation processes are not effective. Spins cross relax for each other and then relax to the lattice via the EQQ interaction. (2) Diffusion region: $11 < T < 16.6$ K, cross relaxation turns off as the lines motionally narrow making relaxation more difficult. However, as the temperature warms, direct processes become more effective.

transfer of energy from the nuclear spins to the lattice is a slow process. Only at temperatures high enough for self-diffusion to play a significant role will there be an effective direct process. At lower temperatures, energy is transferred indirectly using the molecular rotation states as an intermediary. An intramolecular interaction modulated by an intermolecular electric-quadrupole-quadrupole (EQQ) interaction relaxes the nuclear spins to the molecular rotation states. The EQQ interaction is characterized by a rate $\Gamma_{\rm EQQ}$, which is the rate at which EQQ-induced reorientations of the molecules takes place (Δm_J transitions). The molecular rotation states, in turn, relax to the lattice predominantly through a Raman process. Only nuclear spins in $J=1$ molecules (para-D$_2$ molecules in our work) can relax in this manner. Molecules in the $J=0$ state do not have an m_J degeneracy and therefore cannot undergo Δm_J transitions. Nuclear spins in $J=0$ molecules (HD and ortho-D$_2$ in this work) are rather isolated and can only relax either by spin diffusion to the nuclear spins in the $J=1$ molecules or through self-diffusion when the temperature is warm enough.

The molecular rotation states of the $J=1$ molecules relax to the lattice in a time designated T_{JL}. The nuclear spins in the $J=1$ molecules relax to the molecular rotation states in a time $T_{1,J=1}$. The time T_{JL} can be described by the model of Walker and van Kranendonk[16] and is short compared to $T_{1,J=1}$. Therefore, the transfer of energy between the nuclear spins and the molecular rotation states acts as a "bottleneck" in the relaxation process. Consequently $T_{1,J=1}$ is the effective spin-lattice relaxation time for nuclear spins in $J=1$ molecules. The relation between $T_{1,J=1}$ and the observed relaxation time depends on the temperature regime. Below 11 K in the absence of self-diffusion, the direct relaxation time for spins in the $J=0$ molecules ($T_{1,J=0}$) is effectively infinite. The cross relaxation arising from spin diffusion (T_x) is fast compared to $T_{1,J=1}$. At these temperatures the nuclear spins in the $J=0$ molecules cross relax rapidly to spins in the $J=1$ molecules that, in turn, relax to the lattice.

Above 11 K, self-diffusion motionally narrows the resonant lines resulting in an increase in T_x. This raises the observed T_1 with temperature as spin diffusion becomes a less efficient means of transferring energy to the spins in the $J=1$ molecules. The increase in T_x is eventually compensated by a decrease in $T_{1,J=0}$ as self-diffusion begins to provide an effective direct relaxation mechanism for the spins in the $J=0$ molecules. It should be noted that, in HD–n-D$_2$ mixtures as in earlier work[7] on solid D$_2$, T_x is always rapid enough to maintain a common spin temperature resulting in a common T_1. This is true right up until the melt where self-diffusion becomes quite rapid. In contrast, for relaxation in liquid mixtures, T_x is slow enough that the HD, ortho-D$_2$, and para-D$_2$ relax separately as shown in Fig. 2.

A. T_1 in the rigid lattice

Moriya and Motizuki[17] used the assumption that $T_x \ll T_{1,J=1}$ and $T_{1,J=0}$ to calculate that the observed relaxation rate is given by

$$\frac{1}{T_1}=\left[\frac{C_0}{T_{1,J=0}}+\frac{C_1}{T_{1,J=1}}\right]\frac{1}{C_0+C_1} . \tag{1}$$

Here the C's are the "spin heat capacities,"

$$C_i=N_i\hbar^2\omega_0^2 I(I+1)/3k_B .$$

It was argued in the previous section that $T_{1,J=0} \gg T_{1,J=1}$ in which case Eq. (1) reduces to

$$T_{1,J=1}=fT_1 , \tag{2}$$

where $f=2x/(5-3x)$ for a mixture of ortho-D_2 and para-D_2, and $f=x/(1+3x)$ for a mixture of HD–n-D_2. The concentration of para-D_2 is x, and by n-D_2 (normal-D_2), we mean that para-D_2 is one-third of the total D_2 present. In computing these ratios, it has been taken into account that only $\frac{5}{6}$ of the ortho-D_2 has a NMR signal.

Moriya and Motizuki[17] also computed $T_{1,J=1}$ arising from the EQQ interaction for para-D_2. Using a Gaussian approximation for the spectral density function considered valid for $x>0.5$, and taking into account only nearest-neighbor interactions, they obtained

$$T_{1,J=1}=(3.62\Gamma_{\mathrm{EQQ}})x^{1/2}\ \mathrm{sec} . \tag{3}$$

Here Γ_{EQQ} is in K. Γ_{EQQ} has been factored out of the equation since opinions as to its actual value have changed through the years. For $x<0.5$ (the case for all samples in this work), a calculation of $T_{1,J=1}$ is more complicated since the $J=1$ molecules are more separated resulting in a reduced EQQ interaction. It is apparent that, in some limit, the EQQ interaction will be negligible and the $J=1$ molecules will relax as isolated singles. In this limit $T_{1,J=1}$ will have a temperature dependence rather than a concentration dependence. Harris[18] calculated $T_{1,J=1}$ of para-D_2 for moderately low concentrations. Using a statistical model he obtained

$$T_{1,J=1}=13.0\Gamma_{\mathrm{EQQ}}x^{5/3}\ \mathrm{sec} . \tag{4}$$

For very low concentrations Harris[19] speculated that $T_{1,J=1}$ would be proportional to $1/x$. The $1/x$ concentration dependence arises from a Suhl-Nakamura interaction—an indirect process mediated by phonons—rather than an EQQ interaction.

More recent calculations by Fujio, Hama, and Nakamura[20,21] and by Drabold and Fedders[22] have not addressed the problem of para-D_2 explicitly. They have discussed ortho-H_2 relaxing either in a para-H_2 or HD background. In principle, these theories also should apply to the problem addressed here of para-D_2 relaxing in an HD and ortho-D_2 background. Fujio, Hama, and Nakamura used moment methods to calculate relaxation times for all concentration regimes. Drabold and Fedders argue that the statistical model used by Harris is inherently unphysical since it uses a static configuration to model what is essentially a dynamic process. Drabold and Fedders argue that the use of moment methods assumes homogeneous broadening at all concentrations. As the concentration becomes more dilute, isolated spins are not homogeneously broadened.

Drabold and Fedders[22] develop a model for low concentrations in which the phonons drive the concentration-dependent EQQ interaction. The model contains two dimensionless parameters $p_1=\gamma/(x^{5/3}\Gamma_{\mathrm{EQQ}})$ and $p_2=\omega_0/(x^{5/3}\Gamma_{\mathrm{EQQ}})$, where γ is the molecular correlation frequency and ω_0 is the Larmor frequency. These parameters indicate the transitions between different concentration regimes. For $p_1 \gg 1$, the molecules relax as isolated singles regardless of the value of p_2. In this concentration regime, $T_{1,J=1}$ has a temperature dependence because the phonons dominate the relaxation process but there is no concentration dependence. For $p_1 \ll 1$, there are two limiting cases; $p_2 \ll 1$ where $T_{1,J=1}$ is given by

$$T_{1,J=1}\approx\frac{\omega_0^{8/5}}{88.08\omega_d^2\Gamma_{\mathrm{EQQ}}^{3/5}x} , \tag{5}$$

while for $p_2 \gg 1$,

$$T_{1,J=1}\approx\sqrt{8/\pi}\left[\frac{\Gamma_{\mathrm{EQQ}}x^{5/3}}{\omega_d^2}\right] . \tag{6}$$

In these expressions ω_d is the intramolecular coupling frequency which, for deuterons, is $1.58\times10^5\ \mathrm{sec}^{-1}$. To summarize, the Drabold and Fedders model predicts an $x^{5/3}$ concentration dependence for moderately low concentrations with a transition to a $1/x$ concentration dependence as the concentration is lowered. The concentration at which the transition takes place depends on the Larmor frequency. At very low concentrations there is a transition to an isolated singles regime with no concentration dependence. This transition is determined by the molecular correlation frequency. The predicted $1/x$ dependence occurs for entirely different reasons than the prediction by Harris.

B. T_1 in the diffusion region

Bloom[4] examined the proton resonance of HD with H_2 impurities. For small concentrations of $J=1$ molecules ($x \ll 1$), he developed a model to describe relaxation in the diffusion region. Since we are considering the analogous problem for deuterons, we would expect Bloom's model to be useful. Bloom's result is

$$\frac{1}{T_1}=\frac{1}{T_{1,J=0}^d}+\frac{f}{T_x+T_{1,J=1}} . \tag{7}$$

Here $T_{1,J=0}^d$ refers to the direct relaxation of the $J=0$ molecules from self-diffusion, T_x is the cross-relaxation time between the two spin systems and $T_{1,J=1}$ again is the EQQ-induced relaxation time of the $J=1$ molecules. The fraction f is the ratio of the spin heat capacities [$2x/(5-3x)$ for D_2 and $x/(1+3x)$ for an n-D_2–HD mixture]. In the limit of short-cross-relaxation times and long-relaxation times for the spins in the $J=0$ molecules, Eq. (7) reduces to Eq. (2) (the rigid lattice expression relating T_1 and $T_{1,J=1}$).

Weinhaus *et al.*,[7] working with ortho-D_2–para-D_2 mixtures, also used the Bloom model to analyze their results for samples with low concentrations of para-D_2. They presented physical arguments that $T_x = BT_2^d$ where B is a number that is around 6. T_2^d is the contribution to T_2 from self-diffusion. It can be described by an Arrhenius relation $T_2^d = (T_2^d)_0 e^{-E/k_B T}$. Their argument is based on the fact that T_x in the diffusion region also depends on self-diffusion. If the approximation is made that the diffusion of the $J=0$ and 1 molecules are roughly equal, T_x can also be described by an Arrhenius relation. Weinhaus *et al.*[7] argue that a random-walk calculation for an fcc lattice shows $1/T_1^d$ to be proportional to a diffusion constant also described by an Arrhenius relation. Therefore, one can write

$$\frac{1}{T_{1,J=0}^d} = AT_2^d ,$$

where

$$A \propto \frac{1}{(1-x)^2 \omega^2} . \tag{8}$$

In a mixture of ortho-D_2 and para-D_2 with $x = 0.05$ and $\omega/2\pi = 4.7$ MHz, Weinhaus *et al.*[7] estimate $A \approx 0.1$ sec^{-2}. They also assume that a similar relation is valid for an hcp lattice, since that is the structure of D_2 at these temperatures and pressures. Combining Eqs. (7) and (8), we take as a model in the diffusion region

$$\frac{1}{T_1} = AT_2^d + \frac{f}{BT_2^d + T_{1,J=1}} , \tag{9}$$

where T_2^d is given by an Arrhenius relation

$$T_2^d = (T_2^d)_0 e^{-E_{\text{act}}/k_B T} . \tag{10}$$

There are three predictions to note from the model. First, because of the frequency dependence of the A coefficient, Weinhaus *et al.*[7] predict that T_1 in the diffusion region will be longer at higher Larmor frequencies. Second, T_1 also depends on the same thermal activation energy for self-diffusion that governs T_2. Measurements of T_1 and T_2 should yield similar information about the activation energy. Third, T_1 depends on the concentration of $J=1$ molecules (para-D_2) in our samples. In samples with low concentrations, T_1 will have a more dramatic temperature dependence. According to Eq. (9), T_1 can be made arbitrarily long with enough of a decrease in the concentration of $J=1$ molecules.

IV. EXPERIMENT

Pulsed DMR measurements were made at 55 MHz in an 8.5 T superconducting magnet. The spectrometer is described in detail elsewhere.[23] The probe consisted of a long Pyrex capillary tube with a spherical bulb about 6 mm in diameter blown on the end that served as the sample chamber. A solenoid coil with six turns was wound from copper wire and parted in the center so that it could fit around the glass bulb. The leads from the coil were connected to a length of RG-58 coaxial cable that served as the transmission line. A carbon-glass resistor was placed next to the sample chamber for temperature measurements. The melting point of D_2 provided an easy temperature reference and could be determined to within ±0.1 K. A liquid-helium flow cryostat was used to maintain a desired temperature. The temperature was controlled dynamically by adjusting the rate of liquid-helium flow and the current through a heater wire. Temperatures above 11 K could be regulated to ±0.02 K. Between 8 and 11 K, the regulation of temperatures to within ±0.1 K was possible. The regulation of temperatures below 8 K could not be accomplished.

The samples were created by mixing HD and n-D_2 gases in a bottle at room temperature. The gasses were mixed in the desired proportions and then allowed to stand for several weeks to insure that they were well mixed. At the beginning of an experiment the NMR probe was evacuated. A typical pressure reached was between 5 and 15×10^{-6} torr. The probe was then cooled to around 19 K, a temperature just above the 18.7-K triple point of D_2. At this temperature, liquid samples could be created. The gas mixture, from which a sample would be made, would flow into the sample chamber under its own pressure where it would condense. The amount of gas used was calculated to, when liquified, completely fill up the sample chamber. When relatively pure HD or D_2 were being studied, the final pressure would correspond to saturated vapor pressures previously reported[24] for the measured temperature. This indicated that the sample was in the liquid phase and provided a check on the consistency of the temperature measurements. After a wait of several hours for a phase equilibrium to be established, measurements could be performed in the liquid phase. When a solid sample was desired, the temperature would be lowered further but only after a liquid-gas phase equilibrium has been achieved.

The composition of mixture samples could be determined from analysis of NMR spectra in the liquid phase. As mentioned previously, liquid D_2 has a single resonance line slightly offset from the center of the HD doublet. With proper shimming of the magnetic field, a magnet-limited line had a full width at half maximum near 15 Hz. With this resolution all three lines could be distinguished and the sample composition determined from their relative intensities. For the samples with an n-D_2 impurity of less than 10%, DMR separation was difficult and mass spectroscopy was used on the gas mixture to determine the composition. We measured the composition of one sample using both methods and the results were consistent. It was assumed that the composition did not change much when the gas was condensed and frozen. This appeared to be a good assumption for samples that were made from gas mixtures that had been allowed to stand for several weeks. At least two samples were made from each gas mixture and, to within the ±0.01 uncertainty in D_2 concentration associated with the measurement, the composition was the same in each case. In an earlier attempt at the experiment when a gas mixture was used without waiting long enough for it to thoroughly mix, sample compositions were not reproducible. In fact, the composition and T_1's of a solid sample created from a gas mixture that had not been allowed to stand long enough would change from one hour to the

TABLE I. Measurements of T_1 as a function of temperature for n-D_2 and the seven mixture compositions studied.

n-D_2		(65% HD/(35% n-D_2)		(83% HD)/(17% n-D_2)		(88% HD)/(12% n-D_2)		(90% HD)/(10% n-D_2)		(96% HD)/(4% n-D_2)		(97% HD)/(3% n-D_2)		(98% HD)/(2% n-D_2)	
T (K)	T_1 (sec)	T (K)	T_1 (sec)	T (K)	T_1 (sec)	T (K)	T_1 (sec)	T (K)	T_1 (sec)	T (K)	T_1 (sec)	T (K)	T_1 (sec)	T (K)	T_1 (sec)
9.1	8.4	11.4	3.7	9.6	1.3	8.1	1.6	10.2	2.6	7.5	7.1	7.6	17	9.2	22
11.2	8.2	12.0	3.9	9.6	1.4	9.0	1.5	11.1	3.1	8.8	8.0	8.6	14	10.1	20
12.6	8.2	12.9	4.3	10.5	1.4	10.0	1.4	12.0	6.6	9.8	7.8	11.3	29	11.2	28
12.8	8.6	14.0	5.3	10.5	1.1	10.8	1.7	12.9	20	9.9	7.7	12.7	150	12.2	61
13.8	8.5	14.5	7.2	11.8	2.0	11.5	2.2	14.0	71	9.9	7.7	13.0	210	13.0	190
14.7	8.8	15.1	11	11.8	2.1	12.1	5.0	14.9	165	11.0	8.8	13.8	430	14.1	400
15.4	9.6	15.6	17	12.8	5.6	12.5	7.7	15.9	200	11.9	17	13.9	480	15.0	420
15.9	10	15.7	18	12.8	4.8	12.9	14			12.4	34	14.9	580	16.0	315
16.0	11	16.1	28	13.3	9.1	13.2	20			13.0	64	15.8	420		
16.6	13	16.4	32	13.8	19	13.9	47			14.0	210				
16.6	13			13.8	16	14.2	81			15.0	350				
16.7	14			14.1	23	14.9	120			15.8	410				
16.7	13			14.3	32	15.2	180								
17.4	20			14.8	50	15.8	190								
17.7	23			14.9	59	16.0	210								
17.7	26			15.7	120										
17.7	25			16.3	150										
18.2	31			16.4	160										
18.4	48														

next. These nonequilibrium effects had time scales on the order of days. Samples that had been allowed to mix long enough had consistent and reproducible DMR results after cycling between the solid, liquid, and gas phases. Even though HD has a lower triple point (16.6 K), it was found that if the gases were well mixed, no fractional separation between the HD and n-D_2 would occur during phase cycling.

Measurements of T_1 were made by determining the signal intensity from a steady-state sequence of 90° pulses. Variations were made in the repetition interval between the pulses and the resulting variation in signal intensity was fitted to a single exponential recovery function. This pulse sequence was the most time efficient way to proceed for long relaxation times. A few measurements were made using 90°-tau-90° and 180°-tau-90° pulse sequences to check for consistency. In the warm solid, where the linewidths were limited by the magnet, T_2 was measured using a Carr-Purcell-Meiboom-Gill (CPMG) pulse sequence. The resulting echo envelope was fitted to a single exponential decay. When the temperatures were cold enough that echoes could no longer be formed, T_2 was taken to be the decay time of the free induction decay (FID) corrected for the 16 msec decay caused by the magnet inhomogeneity.

V. RESULTS AND DISCUSSION

Tables I and II list the T_1 and T_2 data. Table III lists parameters used in the data analysis. Listed in Table III under the heading measured parameters are the rigid lattice T_1's ($T_{1,\mathrm{rl}}$) and T_2's ($T_{2,\mathrm{rl}}$). These are determined for each sample by averaging the respective T_1 and T_2 values for temperatures between 8 and 11 K. Equation (2) is considered valid in the rigid lattice allowing us to write

$$T_{1,J=1}=(f)T_{1,\mathrm{rl}} \; . \qquad (11)$$

Under the heading calculated parameters in Table III are the spin heat capacity ratios (f) and the $T_{1,J=1}$'s computed from Eq. (11).

Figure 5 compares $T_{1,J=1}$ versus the concentration of para-D_2 for the present experiments (solid squares) and the 4.7-MHz results of Weinhaus *et al.*[7] on para-D_2–ortho-D_2 mixtures (open circles). For the range of concentrations between 0.04 and 0.33, Fig. 5 shows that an $x^{5/3}$ law is a good fit for both sets of data. Fitting the data from the present work in the 0.04–0.33 concentration range to an $x^{5/3}$ law yields

$$T_{1,J=1}=9.0x^{5/3}\ \mathrm{sec} \; . \qquad (12)$$

Equation (12) is plotted in Fig. 5 for comparison to the $T_{1,J=1}$ data. The coefficient of 9.0 is in agreement with the coefficient of 9 obtained for this range of concentrations by Weinhaus *et al.*[7] Evidently the EQQ interaction between the para-D_2 molecules is not affected by replacing ortho-D_2 with HD. Comparison to Eq. (6) indicates that Γ_{EQQ} is 1.1 K. Calculations of Γ_{EQQ} have yielded values of 0.92 (Ref. 25) and 0.81 K.[26] Equation (6) is only

TABLE II. Measurements of T_2 as a function of temperature. Listed with each T_2 result is the method of measurement. CPMG means a Carr-Purcell-Meiboom-Gill echo train. FID means a free induction decay corrected for the magnet inhomogeneity.

n-D_2			(65% HD)/(35% n-D_2)			(83% HD)/(17% n-D_2)			(88% HD)/(12% n-D_2)			(96% HD)/(4% n-D_2)			(97% HD)/(3% n-D_2)		
T (K)	T_2 (msec)	Method	T (K)	T_2 (msec)	Method	T (K)	T_2 (msec)	Method	T (K)	T_2 (msec)	Method	T (K)	T_2 (msec)	Method	T (K)	T_2 (msec)	Method
9.1	0.28	FID	8.9	0.29	FID	9.6	0.33	FID	8.1	0.32	FID	7.5	0.34	FID	7.8	0.35	FID
11.1	0.34	FID	10.5	0.30	FID	9.6	0.30	FID	9.0	0.32	FID	8.8	0.34	FID	8.8	0.35	FID
12.8	0.76	FID	11.4	0.44	FID	10.5	0.39	FID	10.0	0.32	FID	9.8	0.36	FID	11.5	0.67	FID
13.8	2.5	FID	11.4	0.44	FID	10.5	0.39	FID	10.8	0.47	FID	9.8	0.36	FID	15.7	58	CPMG
14.7	5.9	FID	12.0	0.77	FID	11.8	1.1	FID	11.5	0.74	FID	11.0	0.48	FID	16.0	80	CPMG
15.4	11	FID	12.9	2.5	FID	11.8	1.1	FID	12.1	1.4	FID	11.9	0.92	FID	16.3	96	CPMG
16.0	107	CPMG	14.0	3.3	FID	12.8	2.5	FID	12.5	2.1	FID	12.4	4.4	CPMG			
16.6	215	CPMG	14.5	23	CPMG	12.8	2.5	FID	12.9	2.8	FID	13.0	8.6	CPMG			
16.8	230	CPMG	15.1	52	CPMG	13.3	25	CPMG	13.2	3.1	FID	13.4	14	CPMG			
17.7	675	CPMG	15.6	95	CPMG	14.1	32	CPMG	14.2	22	CPMG	14.0	31	CPMG			
18.4	1300	CPMG				14.3	44	CPMG	15.8	60	CPMG	14.4	38	CPMG			
						14.9	72	CPMG	16.0	78	CPMG	14.9	47	CPMG			
						15.7	123	CPMG				15.4	113	CPMG			
												15.8	125	CPMG			
												16.4	131	CPMG			

TABLE III. Parameters used in analyzing the data. The rigid lattice T_1 ($T_{1,\mathrm{rl}}$) and T_2 ($T_{2,\mathrm{rl}}$) are determined for each sample by averaging the measurements between 8 and 11 K of T_1 and T_2. For n-D_2, f is $2x/(5-3x)$ and for the HD–n-D_2 mixtures, f is $x/(1+3x)$, where x is the para-D_2 concentration. $T_{1,J=1}$ is defined by Eq. (11). The activation energies $E_{\mathrm{act}}(T_2)$ and $E_{\mathrm{act}}(T_1)$ are obtained from fits to the T_2 and T_1 data, respectively [see Figs. 8(a)–8(d)]. The scaling factor $B=T_x/T_2$ is determined from Eq. (19).

	Measured parameters		Calculated parameters		Fitted parameters		
Mixture	$T_{1,\mathrm{rl}}$ (sec)	$T_{2,\mathrm{rl}}$ (msec)	f	$T_{1,J=1}$ (sec)	$E_{\mathrm{act}}(T_2)$ (K)	$E_{\mathrm{act}}(T_1)$ (K)	B
n-D_2	8.3	0.28	0.17	1.4	309	310	8
(65% HD)/(35% n-D_2)	3.0	0.30	0.086	0.26	250	259	20
(83% HD)/(17% n-D_2)	1.3	0.32	0.048	0.063	244	268	60
(88% HD)/(12% n-D_2)	1.5	0.32	0.036	0.054	226	262	100
(90% HD)/(10% n-D_2)	2.6		0.030	0.079			
(96% HD)/(4% n-D_2)	7.7	0.34	0.013	0.10			
(97% HD)/(3% n-D_2)	15	0.35	0.0097	0.15			
(98% HD)/(2% n-D_2)	21		0.0065	0.14			

an approximate solution so a deduction of Γ_{EQQ} from it cannot be regarded as exact.

At lower concentrations there is a difference between the two sets of $T_{1,J=1}$ data. This difference is predicted from the Drabold-Fedders theory and reflects the difference in Larmor frequencies at which the two sets of data were taken. At 55 MHz the parameter p_2 is about 1 at a concentration of 0.027, where the 55-MHz data reach a minimum. For 4.7-MHz deuterons p_2 is about 1 at a concentration of 0.0062, much smaller than any of those studied in the work of Weinhaus *et al.*[7] On the low concentration side, a reasonable fit to a $1/x$ law can be made. The fitted curve, also plotted in Fig. 5, is

$$T_{1,J=1}=1.8\times10^{-3}(1/x)\ . \tag{13}$$

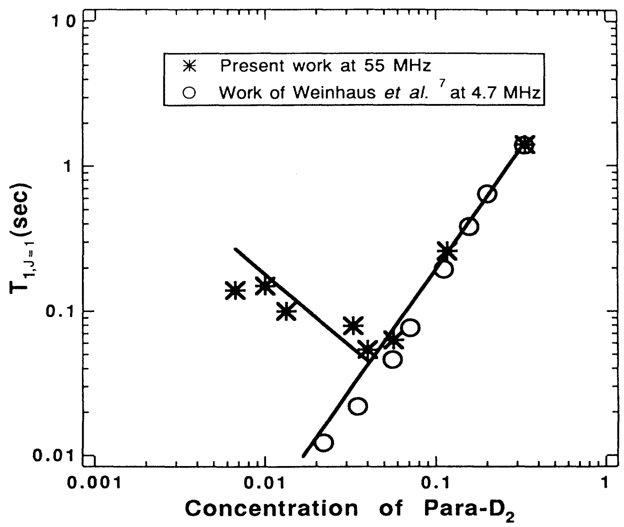

FIG. 5. Comparison of $T_{1,J=1}$ for para-D_2 molecules. The solid squares represent the present work at 55 MHz, the open circles represent the work of Weinhaus *et al.* (Ref. 7) at 4.7 MHz. The two solid lines are the best fits to an $x^{5/3}$ law and a $1/x$ law [Eqs. (12) and (13), respectively] in the concentration regimes that they are expected to apply.

This is in qualitative, but not quantitative, agreement with Eq. (5) which yields

$$T_{1,J=1}=4.2\times10^{-6}(1/x)\ .$$

There are, however, some problems with Eq. (5). First, Eq. (5) predicts $T_{1,J=1}$ to have an $\omega_0^{8/5}$ dependence. Studies of HD with n-H_2 impurities by Hardy and Gaines[5] and Rubins *et al.*[6] have shown a shift of the $T_{1,J=1}$ minimum for different Larmor frequencies but have not observed a frequency dependence of this nature. Second, when p_2 is of order 1 at $x=0.027$, Eqs. (5) and (6) approach different limits. Evaluating Eqs. (5) and (6) at $x=0.027$ for $\Gamma_{\mathrm{EQQ}}=1.1$ yields 1.6×10^{-4} and 2.2×10^{-2} sec, respectively. These equations are not meant to be valid for p_2 of order 1 but it is disturbing that they approach such different limits. The $T_{1,J=1}$ data does not show any discontinuity in switching between different concentration power laws.

The most striking frequency dependence of T_1 occurs in the diffusion region. Figure 6 compares T_1 data for n-D_2 reported by Weinhaus *et al.*[7] (open circles) with the T_1 for n-D_2 reported in this work (solid squares). The results are in agreement until warm temperatures just before the melt. The higher-frequency data make a much sharper increase at warmer temperatures. This result is predicted by the model for T_1 in the diffusion region. In the 4.7-MHz case for n-D_2, the decrease in the relaxation rate that results from slowing spin diffusion is almost exactly matched by an increase in the relaxation rate resulting from self-diffusion. The net result is that, in the diffusion region, T_1 is almost independent of temperature. At 55 MHz, relaxation arising from self-diffusion is inhibited at the higher Larmor frequency. The decrease in the relaxation rate as spin diffusion is slowed is not canceled and the result is an increase in T_1 as the melt is approached.

For samples with lower concentrations if para-D_2, the

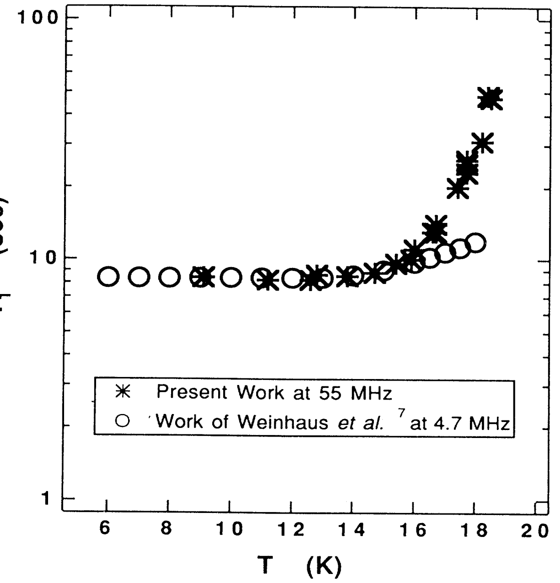

FIG. 6. Comparison of T_1 for n-D$_2$. The solid squares represent the present work at 55 MHz, the open circles represent the work of Weinhaus *et al.* (Ref. 7) at 4.7 MHz.

increase in T_1 at warmer temperatures will be even greater because there are less relaxation centers to which spins can diffuse. Bloom's model for T_1 in the diffusion region, Eqs. (9) and (10), describes the competing effects spin diffusion and self-diffusion have on the overall relaxation rate. The competition can result in maximum in T_1 for low enough para-D$_2$ concentrations and high enough temperatures. The three purest HD samples (96% HD, 97% HD, and 98% HD) have T_1 maxima but they are not at the predicted temperatures. The location of the predicted T_1 maxima can be calculated from Eq. (9) by setting equal to zero the derivative of $1/T_1$ with respect to T_2^d and solving for $(T_2^d)_{T_{1\,\max}}$, the T_2^d for which there will be a maximum in T_1. The result is

$$(T_2^d)_{T_{1\,\max}} = \sqrt{f/BA} - \frac{T_{1,J=1}}{B} \; . \qquad (14)$$

The work of Weinhaus *et al.*[7] reports $A(1-x)^2\omega^2$ to be about 1×10^{14} sec^{-2} and B to be about 6. Taking the 97% HD mixture as an example, from Table III, $f\approx0.01$ and $T_{1,J=1}=0.15$. An evaluation of Eq. (14) with these numbers yields $(T_2^d)_{T_{1\,\max}}=1.3$ sec. Assuming that, in the diffusion region $(T_2^d)_{T_{1\,\max}}\approx T_2$, the longest T_2 in Table II for this mixture is about 100 msec. The maximum in T_1 for the 97% HD mixture occurs when T_2 is no more than 0.050 sec. The 97% HD mixture will melt before T_2 becomes 1.3 sec long. In fact, for all the mixtures studied in this work, at a 55-MHz Larmor frequency, the relaxation rate from self-diffusion AT_2^d is always small compared to the relaxation rate from spin diffusion $f/(BT_2^d+T_{1,J=1})$. For the 97% HD mixture at the longest T_2 of 100 msec, $AT_2^d=8.4\times10^{-5}$ sec^{-1} and

$$f/(BT_2^d+T_{1,J=1})=1.3\times10^{-2}\ \text{sec}^{-1} \; .$$

It may be argued that the estimations of A and B from previous work on ortho-D$_2$–para-D$_2$ mixtures are not entirely valid for HD–n-D$_2$ mixtures. However, inspection of the data reveals another problem with explaining the T_1 maxima. Bloom's model predicts that T_1 can be made arbitrarily long by making the concentration of para-D$_2$ small enough. The three purest samples of HD show increasing values for T_1 in the rigid lattice but no further increase in the maximum value of T_1 in the diffusion region. The finding of an upper limit of the T_1 for solid HD is consistent with the work of Rubins *et al.*[6] They reported that, near the melt, the proton T_1 in solid HD is independent of impurity concentration.

Experimental evidence leads us to believe that an additional relaxation mechanism is present in solid HD and dominates the relaxation at temperatures near the melt. It might be expected that the fraction of HD molecules in the $J=1$ state could provide additional relaxation. The energy difference between the $J=0$ and 1 rotation states for HD is 128 K.[27] Assuming a Boltzmann distribution of rotational states, it would be expected that the concentration of $J=1$ HD molecules at 15 K is about 6×10^{-4}, a number very small compared to the amount of para-D$_2$ present. However, transitions between rotation states are not forbidden in HD leading to the possibility that HD could have an intrinsic relaxation arising from its ability to make transitions to a $J=1$ state. Determination of an intrinsic relaxation for HD has been made by studies of

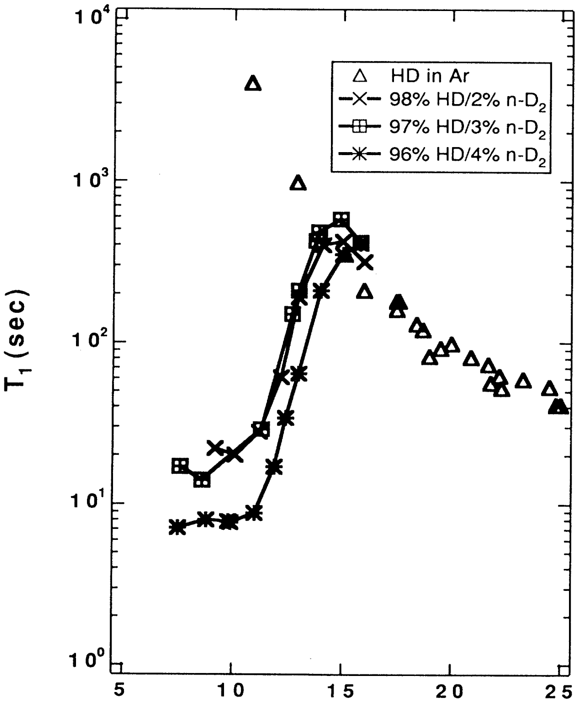

FIG. 7. Comparison of T_1 for the 96% HD, 97% HD, and 98% HD samples with T_1 for HD in argon. Regardless of how low the para-D$_2$ concentration is, the T_1 for solid HD does not become greater than the T_1 for HD in solid argon.

the spin-lattice relaxation of HD isolated in solid argon. Ganem *et al.*[28,29] studied the deuteron relaxation of HD in solid argon at the same Larmor frequency (55 MHz). Figure 7 compares the deuteron T_1's for HD in argon with the T_1's of the three solid HD samples containing the lowest amounts of n-D_2. The T_1 for HD in argon increases rapidly as the temperature is lowered and is independent of the para-D_2 concentration. The para-D_2 present in an HD in argon sample relaxes at a separate, much faster, rate.[28,29] In effect, placing HD and para-D_2 in an argon matrix isolates them from one another and turns off spin diffusion. The situation is similar to that of an HD–n-D_2 liquid mixture where spin diffusion is shut off by rapid motion resulting in separate relaxation times for HD and para-D_2 (see Fig. 2). However, for HD in solid argon, spin diffusion cannot be turned on by lowering the temperature. As a result, T_1 does not decrease at lower temperatures as it does for an HD–n-D_2 mixture. What is interesting though is that over the 14–16.6 K temperature range (where spin diffusion in an HD–n-D_2 mixture is not very effective), T_1 for HD in argon is essentially the same as for the three samples with the highest HD concentrations studied in this work.[28,29] The upper limit on T_1 that the 96% HD, 97% HD, and 98% HD mixtures reach in the 14–16.6 K temperature range is the T_1 for HD in argon.

Contrary to the assumption of Bloom's model that the HD relaxation time at these temperatures is effectively infinite, there is an upper limit on the T_1 for HD determined by its ability to self-relax by becoming a $J=1$ molecule. To account for the intrinsic relaxation of HD we add another relaxation rate to Eq. (9) yielding

$$\frac{1}{T_1}=AT_2^d+\frac{f}{BT_2^d+T_{1,J=1}}+\frac{x_{\mathrm{HD}}}{T_1(\mathrm{HD})}\ , \tag{15}$$

where x_{HD} is the concentration of HD in the mixture. We will assume that $T_1(\mathrm{HD})$ is close to T_1 for HD in argon. Therefore, using the results[29] for the temperature dependence of T_1 for HD in argon, we write, for $T_1(\mathrm{HD})$,

$$\begin{aligned}\frac{1}{T_1(\mathrm{HD})}&=\frac{1}{T_1(\mathrm{HD\ in\ Ar})}\\&=\left[\frac{3e^{-128/T}}{1+3e^{-128/T}}\right]\\&\quad\times\frac{1}{3.0\times10^{-4}(T)^{2.5}}\ \mathrm{sec}^{-1}\ ,\end{aligned} \tag{16}$$

where T is the temperature in Kelvin. We can gain more insight into the meaning of Eq. (15) by performing the following manipulations. First we define a relaxation time T_{1D} arising from the two diffusion processes (spin and self-diffusion) as

$$\frac{1}{T_{1D}}=\frac{1}{T_1}-\frac{x_{\mathrm{HD}}}{T_1(\mathrm{HD})}\ . \tag{17}$$

We also assume that, for our mixtures, our previous argument, that the relaxation rate from self-diffusion is negligible, is true and the AT_2^d term can be neglected. Equation (15) then becomes

$$\frac{1}{T_{1D}}=\frac{f}{BT_2^d+T_{1,J=1}} \tag{18}$$

which, using Eq. (11) for $T_{1,J=1}$ can be written

$$T_2^d=\frac{f}{B}(T_{1D}-T_{1,\mathrm{rl}})\ . \tag{19}$$

In the diffusion region $T_{1D}\gg T_{1,\mathrm{rl}}$ and the contribution to T_2 from the rigid lattice can be neglected, meaning we can approximate T_2^d as T_2. Therefore, Eq. (19) can be approximated as

$$T_2\approx\left[\frac{f}{B}\right]T_{1D}\ . \tag{20}$$

In other words, in the diffusion region we expect that T_1 corrected for the intrinsic relaxation of HD using Eq. (17) and T_2 are directly related to each other by a factor of f/B.

Figures 8(a)–8(d) are plots of $\ln(T_{1D}-T_{1,\mathrm{rl}})$ and $\ln(T_2)$ versus $1/T$ for n-D_2 and the 65% HD, 83% HD, and 88% HD mixtures. In each figure a straight line results for T_2 indicating that an Arrhenius relation, Eq. (10), governs $\ln(T_2)$ and a nearly parallel line results for $\ln(T_{1D}-T_{1,\mathrm{rl}})$ indicating that Eq. (19) is valid. Activation energies for self-diffusion can be obtained from both the T_1 and T_2 data by determining the slopes of the best-fit lines in Figs. 8(a)–8(d). The activation energies as well as the proportionality constant B are listed in Table III under the heading of fitted parameters. An important difference between our mixtures of HD–n-D_2 and the mixtures of ortho-D_2–para-D_2 is that the activation energy for self-diffusion varies with sample composition in HD–n-D_2 mixtures. The activation energy for D_2 (E_{act}) has been reported[10] to be 287 K independent of paraconcentration. For H_2 the reported[2] activation energy is 200 K. Based on these two measurements, E_{act} for HD would be expected to be around 240 K since its mass is intermediate between D_2 and H_2. Measurements for HD vary greatly, Bloom[4] reports 302 K and Rubins *et al.*[6] report 190 K. We expect E_{act} in the mixtures to vary linearly with HD concentration between the value for D_2 and the value for HD. A plot of all the activation energies in Table III versus HD concentration is shown in Fig. 9. Assuming a linear variation of E_{act}, we plot the best-fit line in Fig. 9 which is

$$E_{\mathrm{act}}=308-71x_{\mathrm{HD}}\ \mathrm{K}\ , \tag{21}$$

where x_{HD} is the concentration of HD in the mixture and E_{act} is in K. Extrapolating to $x_{\mathrm{HD}}=0$ yields $E_{\mathrm{act}}=308$ K for pure D_2. The other limit $x_{\mathrm{HD}}=1$ (pure HD) yields $E_{\mathrm{act}}=237$ K. These activation energies are in good agreement with the published values[4,6,10] quoted earlier. The extrapolation of the activation energy for pure HD from the data on the HD mixtures is necessary since the above analysis cannot be performed for the purer HD samples. As shown in Fig. 7, for the 96% HD, 97% HD, and 98% HD mixtures, T_1 near the melt is dominated by the intrinsic relaxation of HD. A T_{1D} for these mixtures cannot be computed from Eq. (17) since diffusion processes are too small a contribution to the overall relaxation rate.

The scaling factor B also varies with the HD concentration. For n-D_2 we find $B=8$, in close agreement with previously reported values of $B=6.5$ and 6.7 for ortho-D_2–para-D_2 mixtures with 2.2 and 7.1 % para-D_2, respectively.[7] However, as the HD concentration in an HD–n-D_2 mixture is raised, we find B to increase as well. As shown in Table III, B increases to 20 for the 65% HD mixture and then up to 100 for the 88% HD mixture.

The factor B relates the cross-relaxation time (T_x) to T_2. Essentially, for a given T_2, cross relaxation between the spins in para-D_2 and HD is much slower than cross relaxation between spins in para-D_2 and ortho-D_2. The cross relaxation between two spin systems depends on the spectral overlap of the resonance lines. For an ortho-D_2–para-D_2 mixture, such as n-D_2, the spectral overlap is very strong since deuterons in ortho-D_2 have essentially the same resonant frequency as those in para-D_2. However, in the diffusion region, the HD resonance line is separating into an eventual 43-Hz-wide doublet (see Fig. 3) while the para-D_2 resonance remains in its original position and finds itself close to the center of the doublet.

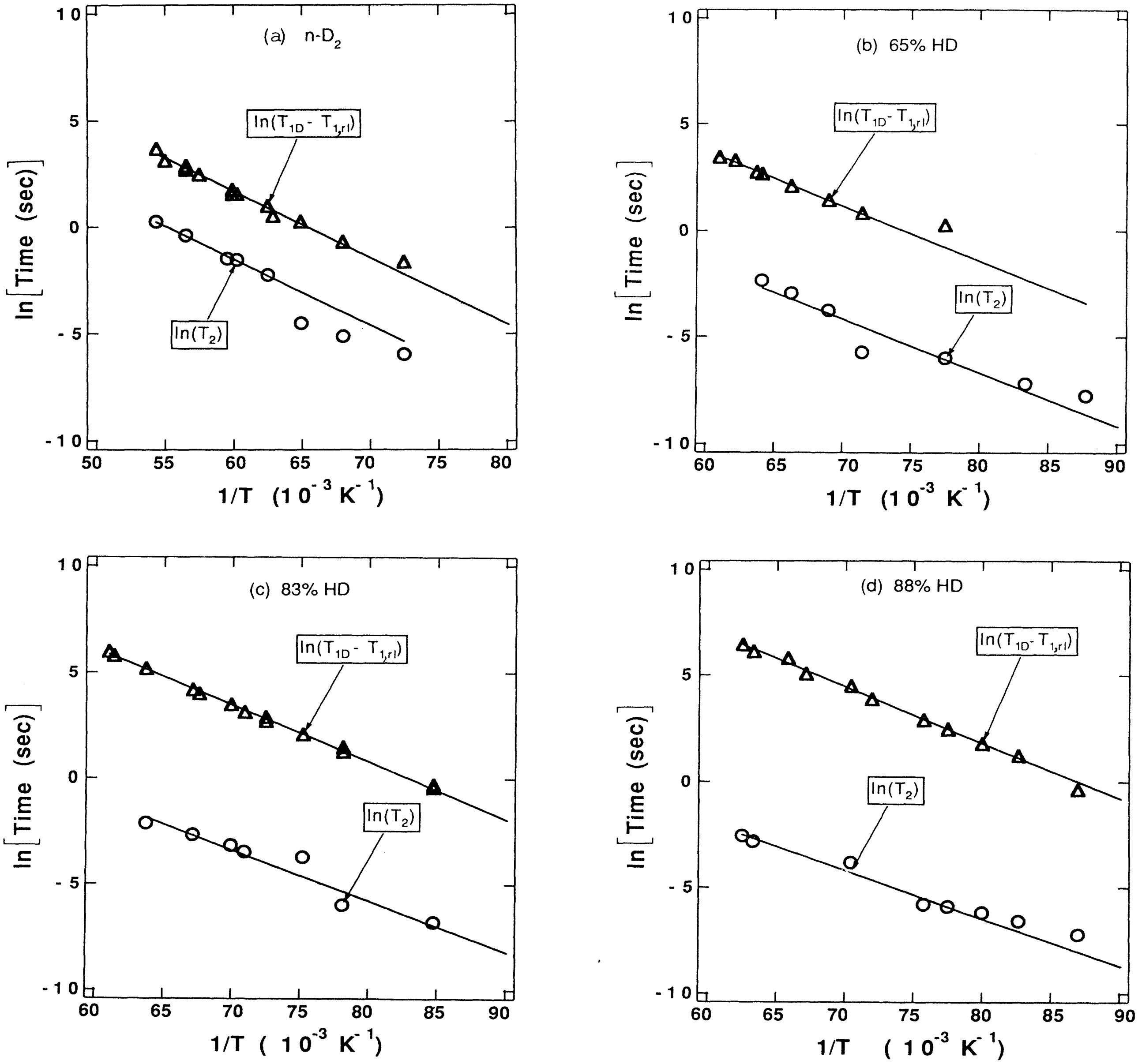

FIG. 8. Plots of $\ln(T_{1D}-T_{1,\mathrm{rl}})$ (open triangles) and $\ln(T_2)$ (open circles) vs reciprocal temperature ($1/T$). The near parallel lines resulting from the fits shown are in agreement with Eq. (19). Table III lists the activation energies obtained from the fits. (a) n-D_2, (b) (65% HD)/(35% n-D_2), (c) (83% HD)/(17% n-D_2), (d) (88% HD)/(12% n-D_2).

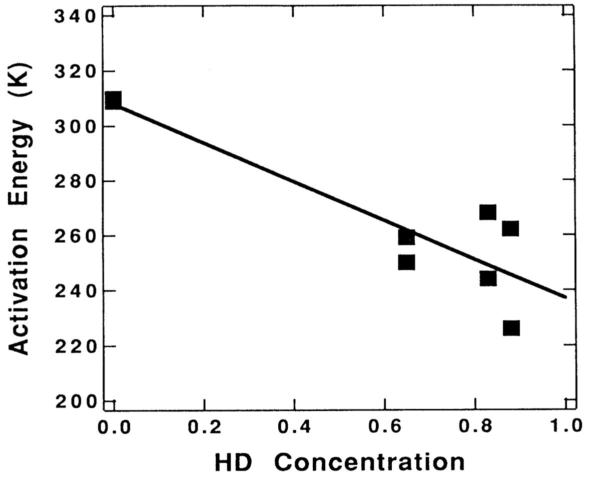

FIG. 9. Activation energies (listed in Table III) are plotted vs HD concentration. The best-fit line $E_{\mathrm{act}}=308-(71)x_{\mathrm{HD}}$ K is drawn. Extrapolating to $x=0$ (pure n-D_2) implies $E_{\mathrm{act}}(D_2)=308$ K. Extrapolation to $x=1$ (pure HD) implies $E_{\mathrm{act}}(\mathrm{HD})=237$ K.

The spectral overlap between the HD and para-D_2 deuteron resonances is greatly reduced resulting in a decrease in the cross-relaxation rate between the spins in the two molecules.

In fact, as a result of the HD doublet formation, the spectral overlap between HD and para-D_2 should be a function of temperature. Treating B as a constant is an approximation. However, the scatter in the T_2 data makes the determination of a functional dependence of B on temperature difficult. An inspection of Figs. 8(b)–8(d) reveals more scatter in the T_2 data than the T_1 data. Part of the reason for the greater scatter for T_2 measurements is the ambiguity in defining T_2 for HD–n-D_2 mixtures. The CPMG pulse sequence regards the HD splitting as an inhomogeneous broadening.[14] Measurements of T_2 at warmer temperatures using the CPMG pulse sequence are not affected by the splitting, but T_2 measurements made from the linewidth are affected. From 14 K to the melting point, the HD resonant structure is broadening, rather than narrowing (see Fig. 3) and in this temperature range, T_2 measurements using a FID which is sensitive to this broadening should yield shorter times than T_2 measurements from a CPMG echo envelope which is not affected by the broadening.

The temperature dependence of the HD resonant structure shown in Fig. 3 is unusual. The reason the structure is narrowing as the temperature is lowered is the effect of the intermolecular proton-proton flip flops. At high temperatures rapid diffusion averages away the intermolecular proton-proton dipolar interaction. The proton flip-flop rate is relatively slow and has little effect on the HD deuteron resonance. The deuteron resonance is split by the scalar intramolecular spin-spin interaction described earlier, with the doublet structure arising from the two distinct orientations of the proton. As the temperature is lowered the proton flip-flop rate increases. A measure of the proton flip-flop rate is the proton T_2 which is 10 msec near the melting point.[4] At 15.4 K the proton T_2 has shortened to about 2 msec and it will shorten further as the temperature drops into the rigid lattice. Eventually the proton-proton flip-flop rate will be fast enough to average out the scalar spin-spin coupling that causes the splitting in the HD deuteron resonance. This is an unusual example of the self-narrowing effect discussed by Abragam[13] and Haeberlen[30] in regards to the silver resonance in silver fluoride (AgF). Another example of the narrowing of a resonant structure split by spin-spin couplings is the proton resonance in ethyl alcohol. The proton resonance in pure ethyl alcohol has a complex multiplet structure arising from various spin-spin couplings. Contamination of the ethyl alcohol with H^+ and OH^- ions alters the shape of the multiplet structure. A sequence of line shapes analogous to Fig. 3 can be created by varying the concentration of the H^+ and OH^- ions. With large enough concentrations, a complete narrowing of the resonant structure into a single line can be accomplished. The narrowing arises from a rapid exchange process involving the hydroxyl proton of the ethyl alcohol molecule that averages away the spin-spin interactions. The rate of exchange can be determined from analysis of the line shape.[31]

The HD self-narrowing effect also explains T_2 in the rigid lattice. The flipping protons effectively remove their influence on the line shape. Consequently, the rigid lattice linewidth shows little dependence on sample composition. Table III shows $T_{2,\mathrm{rl}}$ in all the samples to vary from 0.28 msec in n-D_2 to 0.35 msec in the 97% HD sample. The presence of the protons from the HD has only a slight narrowing effect on the deuteron rigid lattice linewidth. The proton flip flops are too fast for there to be significant broadening.

VI. CONCLUSIONS

In the rigid lattice, para-D_2 concentrations control the HD deuteron spin-lattice relaxation. $T_{1,J=1}$ follows an $x^{5/3}$ law but then makes a transition to a $1/x$ law at a concentration near 0.027 as predicted by the Drabold-Fedders theory.[22] In the diffusion region Bloom's[4] model, modified to account for the intrinsic relaxation of HD, can be used to find a relation between T_1 and T_2. The data show this relation, Eq. (19), to be valid. Activation energies for self-diffusion can be determined from both the T_1 and T_2 results and are in accordance with previous work.[2,4,6,10]

ACKNOWLEDGMENTS

The authors would like to acknowledge helpful conversations with David Drabold, Mark Conradi, and Peter Fedders. Gregory Mohr provided useful advice on experimental details. This work was supported in part by National Science Foundation (NSF) Low Temperature Physics Program Grant Nos. DMR-87-01515 and DMR-90-02857.

*Present address: Department of Physics and Astronomy, University of Georgia, Athens, Georgia 30602.

[1] L. I. Amstutz, H. Meyer, S. M. Myers, and R. L. Mills, J. Phys. Chem. Solids **30**, 2693 (1969).

[2] F. Weinhaus and H. Meyer, Phys. Rev. B **7**, 2974 (1973).

[3] W. P. A. Hass, J. J. Poulis, and J. J. W. Borleffs, Physica (Amsterdam) **27**, 1037 (1961).

[4] Myer Bloom, Physica (Amsterdam) **23**, 767 (1957).

[5] Walter N. Hardy and J. R. Gaines, Phys. Rev. Lett. **17**, 1278 (1966).

[6] R. S. Rubins, A. Feldman, and A. Honig, Phys. Rev. **169**, 299 (1968).

[7] F. Weinhaus, S. M. Myers, B. Maraviglia, and H. Meyer, Phys. Rev. B **3**, 626 (1971).

[8] F. Weinhaus, S. M. Myers, B. Maraviglia, and H. Meyer, Phys. Rev. B **3**, 3730 (1971).

[9] F. Weinhaus, H. Meyer, and S. M. Myers, Phys. Rev. B **7**, 2948 (1973).

[10] F. Weinhaus, H. Meyer, S. M. Myers, and A. B. Harris, Phys. Rev. B **7**, 2960 (1973).

[11] N. J. Poulis and W. P. A. Hass, *Nuclear Magnetic Relaxation* in *Landolt-Börnstein Tables,* edited by K. H. Hellwege (Springer-Verlag, Berlin, 1967), Vol. II, Chap. 9, Sec. **29** 74, p. 7–48.

[12] N. F. Ramsey and E. M. Purcell, Phys. Rev. **85**, 143 (1952).

[13] A. Abragam, *The Principles of Nuclear Magnetism* (Oxford University Press, Clarendon, 1961).

[14] James Richard Beckett, Ph.D. thesis, Rutgers University, 1979 (unpublished).

[15] James R. Gaines and P. C. Souers, Adv. Magn. Reson. **12**, 91 (1988).

[16] J. Van Kranendonk and M. B. Walker, Can J. Phys. **46**, 2441 (1968).

[17] Toru Moriya and Kazuko Motizuki, Prog. Theor. Phys. **18**, 183 (1957).

[18] A. Brooks Harris, Phys. Rev. B **2**, 3495 (1970).

[19] A. Brooks Harris, Phys. Rev. B **1**, 1881 (1970).

[20] M. Fujio, J. Hama, and T. Nakamura, Prog. Theor. Phys. **54**, 293 (1975).

[21] Tuto Nakamura and Motoya Fujio, Prog. Theor. Phys. **54**, 601 (1975).

[22] D. A. Drabold and P. A. Fedders, Phys. Rev. B **39**, 6325 (1989).

[23] Gregory Alan Mohr, Ph.D. thesis, Washington University, 1986 (unpublished).

[24] Harold W. Woolley, Russell B. Scott, and F. G. Brickwedde, J. Res. Natl. Bur. Stand. **41**, 379 (1948).

[25] D. A. Drabold and P. A. Fedders, Phys. Rev. B **39**, 1993 (1989).

[26] J. Hama and T. Nakamura, Prog. Theor. Phys. **44**, 303 (1970).

[27] Isaac F. Silvera, Rev. Mod. Phys. **52**, 393 (1980).

[28] Joseph Ganem, Peter A. Fedders, and R. E. Norberg (unpublished).

[29] Joseph Ganem, Ph.D. thesis, Washington University in Saint Louis, 1989 (unpublished).

[30] Ulrich Haeberlen, *High Resolution NMR in Solids* (Academic, New York, 1976).

[31] James T. Arnold, Phys. Rev. **102**, 136 (1956).